

# Non-local correlation effects and metal-insulator transition in the $s$ - $d$ exchange model

J. Sweep, A. N. Rubtsov<sup>+1)</sup>, M. I. Katsnelson

Radboud University Nijmegen, Institute for Molecules and Materials, NL-6525AJ Nijmegen, The Netherlands

<sup>+</sup>Department of Physics, Lomonosov Moscow State University, 119991 Moscow, Russia

Submitted 22 July 2013

Resubmitted 5 September 2013

The metal-insulator transition within the  $s$ - $d$  exchange model is studied by the Dynamical Mean Field Theory and Dual Fermion approaches. The latter takes into account nonlocal correlation effects which are shown to be essential. In particular, the critical values of the  $s$ - $d$  exchange coupling constant for these two methods turn out to be different by a factor of more than two (for the case of square lattice and spin 1/2 localized electrons). The calculations were performed using a Continuous-Time Quantum Monte Carlo method. The difference of the quantum spin-1/2 case and the classical-spin case is discussed. For the quantum case the sign of  $s$ - $d$  exchange coupling constant is relevant which demonstrates an importance of the Kondo effect.

DOI: 10.7868/S0370274X13190144

The motivation to study the metal-insulator transition in the  $s$ - $d$  exchange, or Vonsovsky–Zener, model [1, 2] (now it is frequently called Kondo lattice model) is given by previous successes obtained studying the metal-insulator transition (MIT) in the Hubbard model [3]. The  $s$ - $d$  exchange model is complementary to the Hubbard model. While in the Hubbard model the interacting electrons responsible for magnetism and for electron conductivity are located in the same band, in the  $s$ - $d$  exchange model they are located in different bands. In one band the electrons are delocalized or itinerant, therefore these electrons are called conduction electrons. The other band contains electrons that are localized on lattice sites. The type of the interaction is also different between the two models. The Hubbard model contains an on-site Coulomb interaction modeled by a single energy parameter  $U$ . The  $s$ - $d$  exchange model contains a spin-spin interaction between the localized and conduction electrons with a coupling constant ( $s$ - $d$  exchange parameter)  $J$ . The  $s$ - $d$  exchange model is used in the description of rare earths, in which  $4f$ -electrons have a very localized nature [4]. The description of colossal magnetoresistance materials such as (La,Ca,Sr)MnO compounds sometimes is based on the  $s$ - $d$  exchange model assuming that the  $t_{2g}$  electrons are rather localized and the  $e_g$  electrons are itinerant [5].

Whereas for relatively weakly correlated systems a crystal with half-filled energy bands is a metal, for strong enough correlation the system should be an insu-

lator, with each electron sitting in a localized state associated with a given site. This corresponds to a splitting of the energy bands into Hubbard subbands separated (for a large enough interaction parameter  $U$ ) by a gap [6, 7]. In the  $s$ - $d$  exchange model the parameter  $U$  is replaced by  $JS$  where  $S$  is the spin of localized electrons. The Hubbard-III approximation [8, 9] provides a qualitative description of the metal-insulator transition for both models. This description however does not take into account all quantum effects; for the case of  $s$ - $d$  exchange model, it turns out to correspond to the classical spin limit  $S \rightarrow \infty$  [9]. The Dynamical Mean Field Theory (DMFT) [10] was a real breakthrough in this respect dramatically improving the description of the metallic phase near the transition. Within the Hubbard-III approximation the main effect of approaching the MIT is a growth of the damping of the electron states at the Fermi energy together with the appearance of shoulders, the precursors of future Hubbard bands (two-peak structure). Within the DMFT a *three*-peak structure is found with the “Kondo”-peak near the Fermi energy, corresponding to a growth of the effective mass instead of a growth of the damping. The origin of this peak is the formation of a resonance due to electron scattering by *quantum* spins [10]. The dynamical mean-field theory is formally exact in the limit of infinite space dimensionality whereas the Hubbard-III approximation is formally exact (within the  $s$ - $d$  exchange model) in the limit of infinite space dimensionality *and* infinite, that is, classical, spin [9]. In particular, in this limit there is no difference between the case of ferromagnetic ( $J < 0$ )

<sup>1)</sup>e-mail: ar@ct-qmc.org

and antiferromagnetic ( $J > 0$ )  $s$ - $d$  exchange coupling; the Kondo resonance exists only in the latter case (a detailed discussion of the Kondo effect and related physics can be found in Ref. [11]).

The DMFT is the best local approximation, that is, it corresponds to an optimal self-consistent choice of the momentum-independent electron self-energy. For real two- and three-dimensional systems it is just an approximation, which is not quite controllable. The Dual Fermion formalism [12–14] allows to construct a diagrammatic expansion for the non-local correlation effects starting from the DMFT Green's function as a zeroth-order approximation. The differences between the Dual Fermion results and the DMFT results were investigated recently [15] for the Hubbard model on a triangular lattice, and turned out to be very essential. The present paper discusses the differences between Dual Fermions and DMFT for the metal-insulator transition in the  $s$ - $d$  exchange model.

The MIT in the  $s$ - $d$  exchange model in the classical limit  $S \rightarrow \infty$  has been studied in Ref. [9]. In this work we consider a *quantum*  $s$ - $d$  exchange model at a two-dimensional (2D) square lattice, for  $S = 1/2$  where we expect quantum effects to be maximal. We study the role of non-local correlation effects by comparison of the results of DMFT and Dual Fermion calculations. We show that the DMFT strongly overestimates the critical value of the coupling constant for the metal-insulator transition  $J_c$ . We also show that in the  $s$ - $d$  exchange model quantum effects are indeed relevant, since the results for positive and negative values of the coupling constant  $J$  are essentially different.

The  $s$ - $d$  exchange model contains electrons that are localized on lattice sites, and conduction electrons that can hop between different sites  $i, j$ . The exchange interaction (with strength  $J$ ) works between the localized and conduction electrons. Let us introduce the annihilation operators  $c_{i\sigma}$  for the conduction electrons,  $\sigma = \uparrow, \downarrow$  is the spin projection. The annihilation operators for the localized electrons will be designated  $d_{i\sigma}$ . The Hamiltonian contains (in order of appearance in Eq. (1)) a hopping term for the conduction electrons, a Hubbard term that works between the localized electrons which is included for calculational purposes to ensure half-filling of the lattice sites, the  $s$ - $d$  exchange interaction between localized and conduction electrons, and the chemical potential  $\mu$  term:

$$H = - \sum_{ij\sigma} t_{ij} (c_{j\sigma}^\dagger c_{i\sigma}) - \sum_i U (n_{i\uparrow} - n_{i\downarrow})^2 + J \sum_{i\sigma} \mathbf{S}_i \cdot \mathbf{s}_i + \mu N, \quad (1)$$

where  $N$  is the number of conduction electrons and  $n_{i\sigma} = \sum_\sigma d_{i\sigma}^\dagger d_{i\sigma}$ . The subscript  $l$  refers to the localized electrons. The spin-spin interaction term reads:

$$J \mathbf{S}_i \cdot \mathbf{s}_i = \frac{J}{4} (n_{l\uparrow} - n_{l\downarrow})(n_{c\uparrow} - n_{c\downarrow}) + \frac{J}{2} d_{l\downarrow}^\dagger d_{l\downarrow} c_{l\downarrow}^\dagger c_{l\downarrow} + \frac{J}{2} d_{l\uparrow}^\dagger d_{l\uparrow} c_{l\uparrow}^\dagger c_{l\uparrow}, \quad (2)$$

where  $n_{c\sigma} = c_{l\sigma}^\dagger c_{l\sigma}$ . The subscript  $c$  refers to the conduction electrons.

The Hubbard interaction is included to (computationally) ensure the homopolarity of the lattice sites (exactly one localized electron per site). Strictly speaking, it is reached only in the limit  $U \rightarrow \infty$ . We will do the calculations for a large but finite  $U$ . Since a number of localized electrons at each site is conserved, the conditions  $\beta U \gg 1$  and  $U \gg J$  exponentially suppress the contribution from states with zero or two localized electrons, thus delivering the  $s$ - $d$  limit. There is a note that these conditions are much weaker than what is required, for example, to obtain the  $t$ - $J$  limit from the single-band Hubbard model [3], where the electrons are not fully localized and one should require  $U$  much larger than the value hopping times the coordination number.

Our goal was to study the density of conduction-electron states (DoS) of the  $s$ - $d$  exchange model at different coupling constants  $J$ . The calculations were carried out at the Matsubara axis (imaginary frequencies). To obtain the densities of states we performed an analytical continuation of the Green's functions on the real axis using the Maximum Entropy method [16, 17]. The Green's functions we obtained self-consistently in both DMFT and in the Dual Fermion approach. In short, both DMFT and Dual Fermion utilize an effective-medium concept, so that they deal with the impurity model described by the action  $S_{\text{imp}} = S_{\text{at}} + \Delta_\omega c_{j,\omega}^\dagger c_{\omega,j}$ , where  $S_{\text{at}}$  is the action of an isolated lattice site, and  $\Delta$  is a hybridization by the effective bath. The frequency-dependence of the hybridization allows to handle the effects of local fluctuations, that underlie the Kondo physics. On the other hand, this  $\omega$ -dependence makes the impurity problem non-hamiltonian and therefore requires the usage of numerical solvers to obtain its Green's function  $g_\omega$  and the two-particle vertex  $\gamma^{(4)}$  (the latter is required for Dual Fermions).

Compared to the initial lattice Hamiltonian (1), the impurity problem allows a much more effective numerical treatment, because the serial expansions for Green's function of a finite-size system can be efficiently estimated. We used the interaction-expansion continuous-time quantum Monte Carlo procedure (CT-QMC) [18, 19] as a numerical solver. The code is based

on the expansion in powers of  $U(n_{l\uparrow} - \alpha_{\uparrow})(n_{l\downarrow} - \alpha_{\downarrow}) + J(\mathbf{S} - \boldsymbol{\alpha}_l)(\mathbf{s} - \boldsymbol{\alpha}_c)$ . The series is constructed for the partition function (not for its logarithm), so that the connectivity theorem is not used, and one deals with the summation of *non-connected* diagrams. Such series are known to converge for a fermionic impurity problem, and a proper choice of numerical parameters  $\alpha$  makes all the serial terms (almost) positive. The later allows to perform a Markov walk in the space of perturbation terms and thus a stochastic evaluation of the Green's functions. More details about weak-coupling CT-QMC with off-diagonal interaction can be found in [20].

The Dual fermion lattice Green's function equals (spin and orbital indices are omitted)

$$G_{\omega,k} = \frac{1}{(g_{\omega} + g_{\omega} \tilde{\Sigma}_{\omega k} g_{\omega})^{-1} + \Delta_{\omega} - \epsilon_k}, \quad (3)$$

where  $\epsilon_k$  is a dispersion law arising from the hopping  $t_{ik}$  and  $\tilde{\Sigma}$  is the self-energy function of the dual ensemble obtained in a certain diagrammatic approximation. The vertices of the dual diagrams are the vertex parts of the impurity problem. DMFT can be represented as the zeroth-order Dual Fermion scheme with  $\tilde{\Sigma} = 0$ . In this approximation, the lines (propagators) in the dual diagrams have a simple meaning: they are equal to the non-local part of the Green's function,  $\tilde{G}_{\omega,k}^{\text{DMFT}} = G_{\omega,k} - G_{\omega,r=0}$  (for a general case,  $\tilde{G}$  and  $G$  are also exactly related, although the relationship is more complicated). One can easily see that DMFT describes the purely local contribution to the lattice self-energy (and it is actually shown to correspond to the summation of all local diagrams), whereas the Dual Fermion diagrams describe non-local effects. More technical detail can be found in Ref. [12] in which explicit calculations are performed on the Hubbard model and in Ref. [13] which shows the general applicability of the Dual Fermion approach.

The hybridization function  $\Delta_{\omega}$  was obtained self-consistently from the condition that the local part of the dual propagator vanishes,  $\tilde{G}_{\omega,r=0} = 0$ . This eliminates the first-order Hartree dual diagram, and thus the leading correction to  $\tilde{\Sigma}$  is given by the second-order (see diagram b and formula (20) of Ref. [13]),

$$\tilde{\Sigma}_{\omega,r} = \frac{1}{2\beta^2} \sum_{\omega+\omega_2=\omega'+\omega'_2} \gamma_{\omega\omega'\omega_2\omega'_2}^{(4)} \tilde{G}_{\omega'r} \tilde{G}_{\omega_2r} \tilde{G}_{\omega'_2r} \gamma_{\omega'\omega\omega_2\omega_2}^{(4)} \quad (4)$$

(summation over the spins is also implied).

In short, all local interactions (containing  $J$ ) are captured in the calculation of the local Green's function by CT-QMC, and the non-local corrections through the dual diagrams that contain powers of the vertex  $\gamma^{(4)}$  together with the non-local part of the Green's function

that is obtained self-consistently using the hybridization  $\Delta$ .

The last expression (4) is the approximation used for the Dual Fermion calculations in this paper. The calculations were performed for the paramagnetic state of the Hamiltonian (1) on a square lattice with the nearest-neighbor hopping parameter  $t = 0.25$  (which means a half-bandwidth equal to 1), we have chosen  $U = 5$  and the inverse temperature  $\beta = 10$ . The dual fermion diagrams were calculated at a  $24 \times 24$  slab in momentum space.

The final accurate calculations took about two weeks of CPU load per  $J$ -value in the DMFT case and about 10% more in the Dual Fermion case. The amount of self-consistency loops was roughly 10–20 while the number of Monte Carlo steps was roughly doubled with each loop in the last 6 loops until it reached  $8 \cdot 10^8$ .

Let us start with the discussion of the results with the values for metal-insulator transition for the  $s$ - $d$  exchange model. The presence of the transition is visible from Fig. 1.

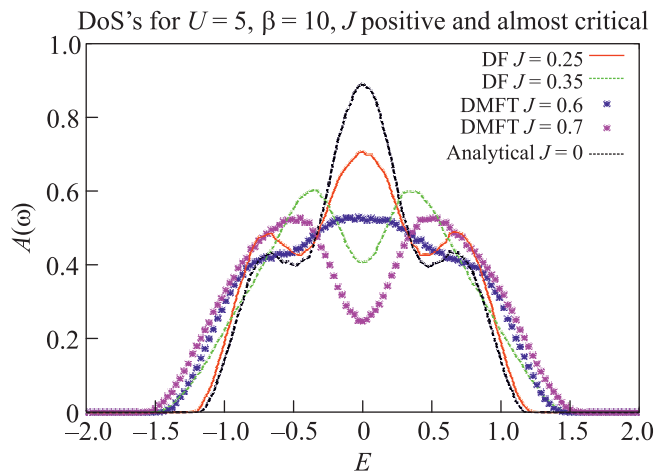


Fig. 1. The DoS around the critical values of  $J$ . The stars correspond to DMFT results, the lines are Dual Fermion calculations. We see the metal-insulator taking place as the local maximum (peak) at the Fermi level ( $E = 0$ ) disappears for higher  $J$ -values. The values are chosen such that they are just around the transition for the two calculational schemes, DMFT and Dual Fermions. For DMFT the value  $J_c \approx 0.65$ , and for the Dual Fermion calculation it gets as low as  $J_c \approx 0.3$

We have quoted values of the coupling constant just around the transition. Although the temperature is quite high and the Hubbard- $U = 5$  we still see a qualitatively correct picture of the densities of states, accurate enough to estimate a reasonable value of the coupling constant  $J$  for the metal-insulator transition.

**Critical values of  $J$  for the metal-insulator transition in different approaches**

Method	$J_c$	Features
Simple self-consistent [9]	0.816	Solution of Heisenberg equation of motion, classical limit: $S \rightarrow \infty$
Hubbard-III [9]	$\approx 0.8$	Inclusion of scattering corrections
DMFT (this work)	$\approx 0.65$	Quantum calculation, local correlations
Dual Fermions (this work)	$\approx 0.3$	Quantum calculation, fermionic non-local corrections

We consider the state to be conducting if there is a local maximum at the Fermi level and insulating if there is a local minimum at the Fermi level, because the temperature is so high.

The choice of  $U = 5$  in the Quantum Monte Carlo calculations is justified because in our calculations  $\beta U = 50 \gg 1$  and  $|U/J| \geq 7$  so that a homopolar state with exactly one localized electron per site is achieved to sufficient extent.

In Table we compare several different calculational methods that were used to obtain a critical value of the coupling constant for the metal-insulator transition.

The difference in behavior of the DoS between positive and negative values of the coupling constant is displayed in Figs. 2 and 3.

In Fig. 2 we display the results for  $|J| = 0.4$  calculated within both DMFT and Dual Fermions. The dif-

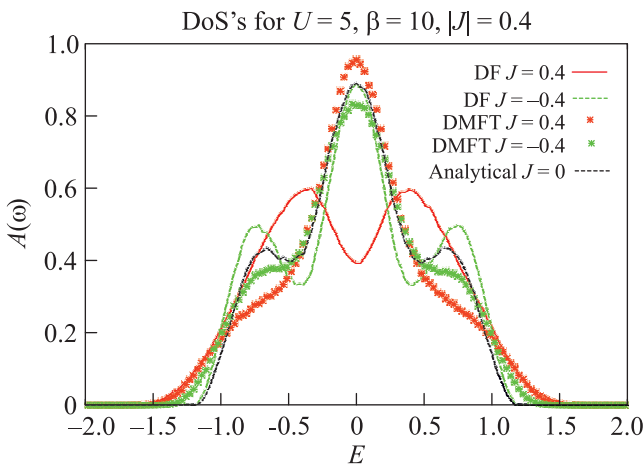


Fig. 2. DoS's for  $|J| = 0.4$ . There is a difference for positive and negative  $J$ . For the local theory, DMFT (stars), the difference is already visible. Beyond this approximation, incorporating non-local correlations using the Dual Fermion approach (lines), it is more pronounced

ferent colors represent positive and negative  $J$ -values. Stars correspond as before to the DMFT-calculation while the Dual Fermion result is drawn with lines. In this picture we look at the general shape of the curves. We see that they are not the same for positive and negative  $J$  and that incorporating non-local corrections through

Dual Fermions changes the results: the difference is more pronounced in the Dual Fermion case.

In Fig. 3 we display the results for  $|J| = 0.7$ , also calculated using DMFT (stars) and Dual Fermions (lines).

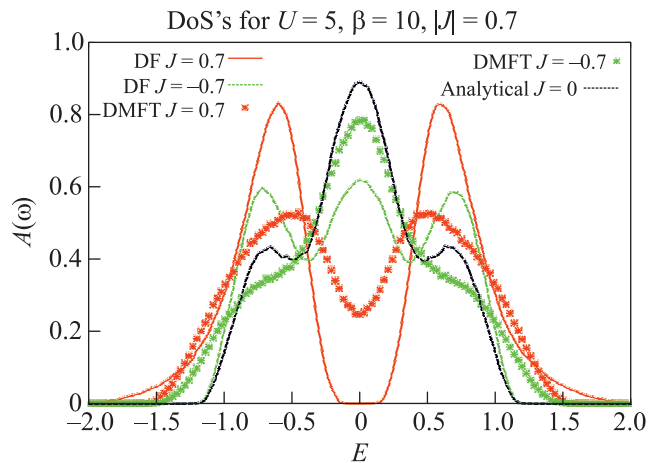


Fig. 3. DoS's for  $|J| = 0.7$ . In this regime the difference between positive and negative  $J$  is clearly visible in both the local (DMFT, stars) and the non-local (Dual Fermion, lines) approaches

The different colors again represent the positive and negative  $J$ -values. The general shape of the curves is much more different between positive and negative  $J$  for  $|J| = 0.7$  than for  $|J| = 0.4$ .

To conclude, in this work we justify the two claims. First, the Dual Fermion formalism description of the metal-insulator transition in the  $s$ - $d$  exchange model to date predicts a critical value of the coupling constant  $J_c \approx 0.3$ . This value differs from the DMFT-result by a factor of more than 2 and corresponds nicely to the result obtained in the other work using a non-local correlations approach [21]. The different results between various calculational schemes are summarized in Table.

Second, there is a clear qualitative difference between densities of states of the  $s$ - $d$  exchange model for antiferromagnetic and ferromagnetic  $s$ - $d$  exchange coupling. This shows that incorporating quantum effects such as the Kondo effect is essential for a good description of the model.

The results in this work were part of the Master's thesis work of JS. The Dual Fermion code was used with kind permission from H. Hafermann. The authors thank A. Lichtenstein for hospitality and fruitful discussions during their stay in Hamburg.

1. S. V. Vonsovsky, *ZhETF* **16**, 981 (1946).
2. C. Zener, *Phys. Rev.* **81**, 440 (1951).
3. J. Hubbard, *Proc. R. Soc. A* **276**, 238 (1963).
4. S. V. Vonsovsky, *Magnetism*, Wiley, New York, 1974.
5. E. L. Nagaev, *Phys. Rep.* **346**, 387 (2001).
6. N. F. Mott, *Metal-Insulator Transition*, Taylor and Francis, London, 1974.
7. M. Imada, A. Fujimori, and Y. Tokura, *Rev. Mod. Phys.* **70**, 1039 (1998).
8. J. Hubbard, *Proc. R. Soc. A* **281**, 401 (1964).
9. A. O. Anokhin, V. Yu. Irkhin, and M. I. Katsnelson, *J. Phys.: Cond. Mat.* **3**, 1475 (1991).
10. A. Georges, G. Kotliar, W. Krauth, and M. J. Rozenberg, *Rev. Mod. Phys.* **68**, 13 (1996).
11. A. C. Hewson, *The Kondo Problem to Heavy Fermions*, Cambridge Univ. Press, Cambridge, 1993.
12. A. N. Rubtsov, M. I. Katsnelson, and A. I. Lichtenstein, *Phys. Rev. B* **77**, 033101 (2008).
13. A. N. Rubtsov, M. I. Katsnelson, A. I. Lichtenstein, and A. Georges, *Phys. Rev. B* **79**, 045133 (2009).
14. A. N. Rubtsov, M. I. Katsnelson, and A. I. Lichtenstein, *Ann. Phys. (N.Y.)* **327**, 1320 (2012).
15. A. E. Antipov, A. N. Rubtsov, M. I. Katsnelson, and A. I. Lichtenstein, *Phys. Rev. B* **83**, 115126 (2011).
16. M. Jarrell and J. E. Gubernatis, *Phys. Rep.* **269**, 133 (1996).
17. A. W. Sandvik, *Phys. Rev. B* **57**, 10287 (1998).
18. A. N. Rubtsov, V. V. Savkin, and A. I. Lichtenstein, *Phys. Rev. B* **72**, 035122 (2005).
19. E. Gull, A. J. Millis, A. I. Lichtenstein et al., *Rev. Mod. Phys.* **83**, 349 (2011).
20. E. Gorelov, T. O. Wehling, A. N. Rubtsov et al., *Phys. Rev. B* **80**, 155132 (2009).
21. S. Capponi and F. F. Assaad, *Phys. Rev. B* **63**, 155114 (2001).